



HAL
open science

Augmented Aircraft Performance by the use of 2 Morphing Technology for a Turboprop Regional Aircraft Wing 4

Frédéric Moens

► **To cite this version:**

Frédéric Moens. Augmented Aircraft Performance by the use of 2 Morphing Technology for a Turboprop Regional Aircraft Wing 4. 2019. hal-02262363

HAL Id: hal-02262363

<https://hal.science/hal-02262363>

Preprint submitted on 2 Aug 2019

HAL is a multi-disciplinary open access archive for the deposit and dissemination of scientific research documents, whether they are published or not. The documents may come from teaching and research institutions in France or abroad, or from public or private research centers.

L'archive ouverte pluridisciplinaire **HAL**, est destinée au dépôt et à la diffusion de documents scientifiques de niveau recherche, publiés ou non, émanant des établissements d'enseignement et de recherche français ou étrangers, des laboratoires publics ou privés.



1 Article

2 Augmented Aircraft Performance by the use of 3 Morphing Technology for a Turboprop Regional 4 Aircraft Wing

5 Frédéric Moens ¹

6 ¹ ONERA ; frederic.moens@onera.fr

7 * Correspondence: Frederic.moens@onera.fr; Tel.: +33-1-4673-4211

8 Received: date; Accepted: date; Published: date

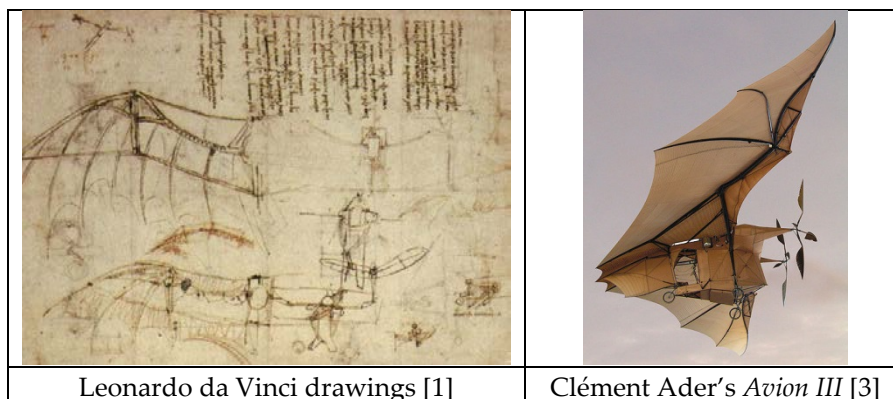
9 **Abstract:** This article presents some application of the morphing technology for aerodynamic
10 performance improvement of turboprop regional aircraft. It summarizes the results obtained in the
11 framework of Clean Sky 2 REG-IADP AIRGREEN2 program on the development and application
12 of dedicated morphing devices for take-off and landing, and their uses in off design conditions. The
13 wing of the reference aircraft configuration considers Natural Laminar Flow characteristics. A
14 deformable leading edge morphing device (“drooped nose”) and a multi functional segmented flap
15 system have been considered. For the drooped nose, the use of deformable compliant structure was
16 considered, as it allows a “clean” leading edge when not used, which is mandatory to keep NLF
17 properties at cruise. The use of a segmented flap makes possible to avoid external flap track
18 fairings, which will lead to performance improvement at cruise. An integrated tracking mechanism
19 is used to set the flap at its take-off optimum setting, and then, morphing is applied in order to
20 obtain high performance level for landing. Finally, some performance improvements can be
21 obtained in climb conditions by using the last segment of the flap system to modify the load
22 distribution on the wing in order to recover some extended laminar flow on the wing upper
23 surface.

24 **Keywords:** morphing; drooped nose, flap; NLF wing;

25

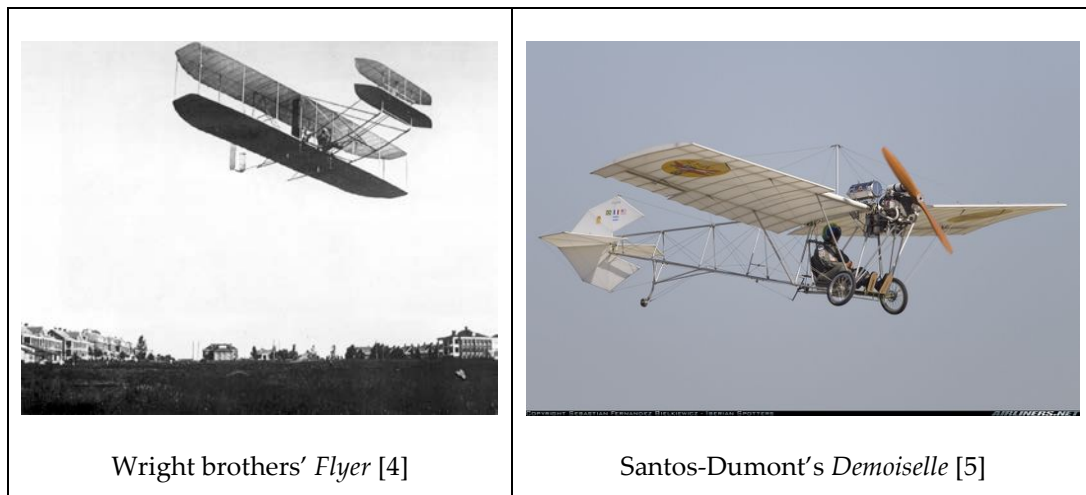
26 1. Introduction

27 Since the beginning of the aviation history, the use of deformable surfaces for controlling the
28 flight is present. The most famous example is the Ader’s Eole airplane which design was inspired by
29 analogy of bat or bird wings (or Leonardo da Vinci drawings).
30



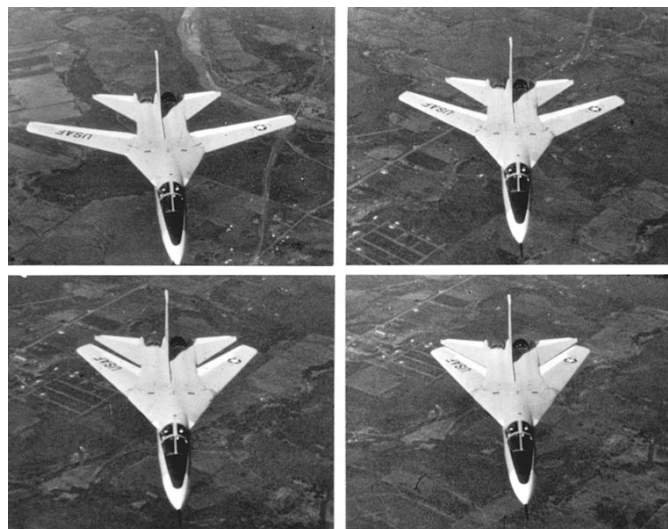
31 **Figure 1 :** How to fly? First ideas.

32 Surface shape modification by the use of flexible structures was used for flight control for most
 33 of the airplanes at this period. However, due to the increase of flight speed, and consequently of the
 34 dynamic pressure in flight conditions, these structures appear to be fragile and need to be reinforced,
 35 leading to a dramatic increases of the weight of the deformation system. The use of rigid structures
 36 in combination with surface control elements became the standard. Note that strictly speaking, the
 37 use of an aileron for flight control or the deployment of flaps or slats at take-off or landing phases
 38 can be considered as “morphing”: the shape of the wing is modified in order to improve its
 39 performance for a flight “off design” condition. Nowadays, a shape is considered as morphed if it
 40 considers deformation of the initial surface by the use of flexible materials or mechanical systems.
 41



42 **Figure 2 :** Pioneer ages – Use of morphing for flight control surface.

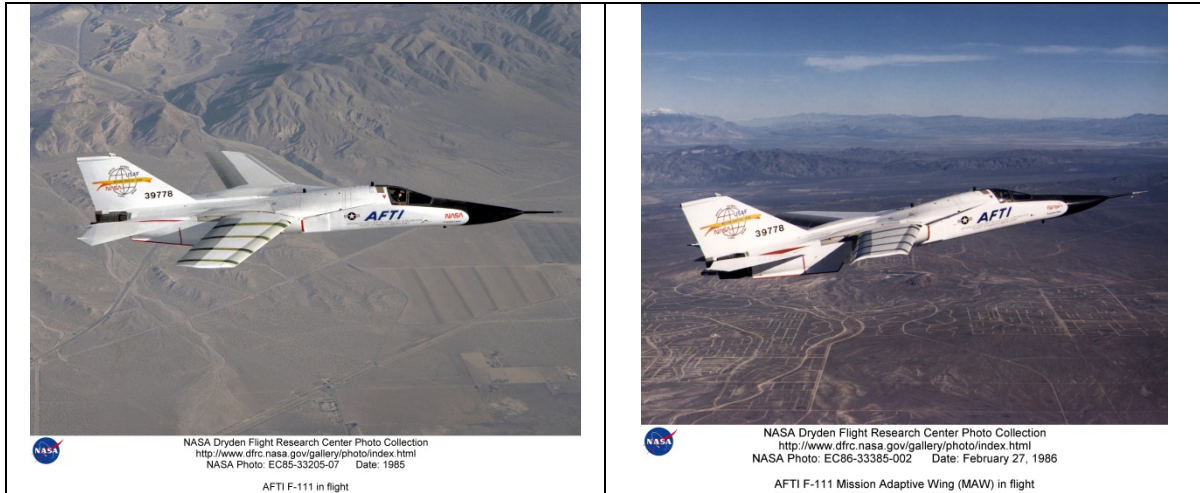
43 Introduction of morphing technology on military aircrafts have shown significant performance
 44 improvements on a large spectrum of flight conditions. For instance, the use of variable swept wing
 45 of supersonic aircrafts to improve performance at transonic or low speed conditions, is a good
 46 illustration (Figure 3).
 47



48
 49 **Figure 3:** F-111 Aircraft wing sweep modification sequence [6].

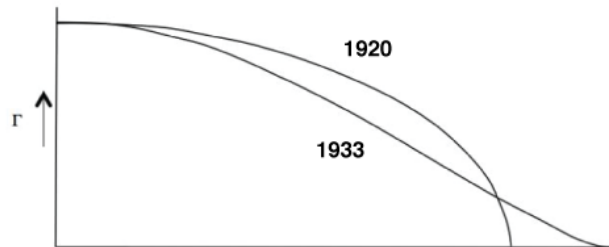
50 In the Advanced Fighter Technology Integration (AFTI) program, by NASA and USAF, the
 51 F-111 wing was equipped with control surfaces so that the airfoil camber was modified and
 52 monitored during flight (Figure 4), and flight tests confirmed significant gain in aerodynamic
 53 performance compared to the reference wing [7].

54



55 **Figure 4 :** AFTI/F-111 aircraft in flight [8] with variable camber wing.

56 However, we have to take care when we extrapolate potential benefits for transport aircraft
 57 applications, for which flight conditions to be considered are more limited. For these applications,
 58 the introduction of multi point MDO process in the design has led to highly efficient design and
 59 it is quite difficult to expect some significant extra gains. For instance, the possibility to play on load
 60 distribution by variable twist technique in order to match the elliptic span loading distribution is
 61 often presented as a good point for the use of morphing technology. However, for transonic aircraft
 62 for which wing flexibility has to be taken into account, it is known that the optimum span loading
 63 considering aero-structural optimization is not elliptic (Figure 5), and is found by MDO processes.



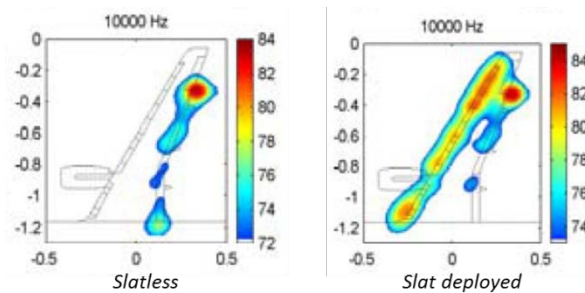
64 **Figure 5 :** Optimal span load distribution for minimum drag [9] from Prandtl's studies. No
 65 constraints: elliptic shape (1920) – Wing with the same structural weight: bell-shaped
 66 (1933).
 67

68 On the other hand, for subsonic aircrafts, such as turboprop, the trapezoidal unswept wing
 69 shape generates naturally a quasi-elliptic span loading. It is therefore very difficult to significantly
 70 improve the lift induced drag component for a well optimized airplane around its design point.

71 However, optimization based on fuel consumption and weight minimization lead generally to
 72 solutions that are much more sensitive to off-design conditions. The use of morphing technology on
 73 wings can help to improve performance for these off design conditions (climb, high speed) or to
 74 extend the flight domain (buffet alleviation, load control, response to gust), as described in the
 75 famous article from Hilbig and Koener [10]. It is also possible to use morphing technology on surface
 76 control such as aileron or on rudder to replace the current mechanisms based on rotation of a rigid
 77 shape.

78 A final application of morphing technology by the use of deformable surfaces is noise reduction.
 79 It is known that major acoustic sources are located at surface discontinuities (slat and flap ends,
 80 Figure 6) and the use of continuous surface will suppress the noise emission at these locations. For
 81 instance, tests carried out by NASA on a business jet configuration (Figure 7) will certainly show
 82 significant noise reduction when compared with the reference plane. However, a global

83 performance assessment has to be stated because for some cases, the existence of discontinuities
 84 helps for aerodynamic efficiency. For instance, for high lift configurations, a slotted flap is much
 85 more efficient than a plain flap, and sometime, some vortices are created in order to improve
 86 maximum lift (slat/fuselage junction or nacelle strakes).
 87



88

89

90

Figure 6 : Acoustic sources identifications on an A321 model in landing configuration (from [11]).



91

92

Figure 7: ACTE flaps on NASA's Gulfstream III aeronautical test bed [12].

93 Finally, at the end of the design process, there is to verify if the gain in aerodynamic
 94 performance is not balanced by an increase of weight due to the system itself or the structure
 95 enforcements.

96 All the pre-mentioned benefits provided by the use morphing technology are for high speed
 97 flight conditions. However, the use of morphing technology at low speed can also be the source of
 98 significant performance improvements. As already mentioned, high lift devices can be considered as
 99 belonging to the family of morphing systems, and the performance level obtained by a system made
 100 of a single slotted Fowler flap and a slotted leading edge slat is almost the maximum achievable level
 101 without active flow control. The drawback is that heavy complex mechanisms are necessary to set
 102 the elements at their position. And when stowed, some external fairings are considered to hide the
 103 mechanics in order to minimize both friction and lift induced drag components in cruise conditions.
 104 However, the selection of a high lift system depends on the performance required for take-off or
 105 landing conditions, the main one being the maximum lift and the stall angle. And the specificity of
 106 high lift systems is that depending on the needs, one system has to be used [13]: If there is a need to
 107 increase the stall angle of attack, a leading-edge device has to be used; if the need is to increase lift at
 108 a given flight angle, the use of trailing edge device is necessary. For both cases, morphing technology
 109 can be considered. Among the different well known leading edge devices, the droop nose is a good
 110 candidate for the application of morphing technology by the use of compliant deformable structures
 111 [16][17]. For trailing edge devices, the use of twistable segmented flaps can be used to increase the
 112 deflection at a fixed global position [19]. Additionally, when flap is stowed, the last segment can be
 113 used in high speed conditions to optimize the wing twist or load distribution. And, last but not least,

114 if the actuation system can be hosted into the wing airfoil shape without external fairing, a
 115 significant drag reduction will be achieved for high speed conditions.
 116



117 **Figure 8 :** Example of airplanes with Flap Track Fairing (FTF) that lead to significant extra
 118 drag at cruise conditions. Image from [14][15].

119 Such application of morphing technology to improve low speed performance has been
 120 evaluated in the framework of the Airgreen 2 EU funded program. This program considers a
 121 regional turboprop aircraft configuration for which Natural Laminar Flow (NLF) technology has
 122 been considered for the design. This article presents the main outcomes of the use of morphing
 123 technology for advanced high lift systems designed on this NLF wing in order to reach the
 124 performance level required. In a second phase, the use of the flap deformation system in climb
 125 conditions has been considered for performance enhancement in this flight condition.

126 3. Baseline configuration

127 The reference aircraft considered is a 90-pax turboprop configuration (Figure 9) designed by
 128 Leonardo Company in the framework of CleanSky 1 GRA-ITD program.
 129

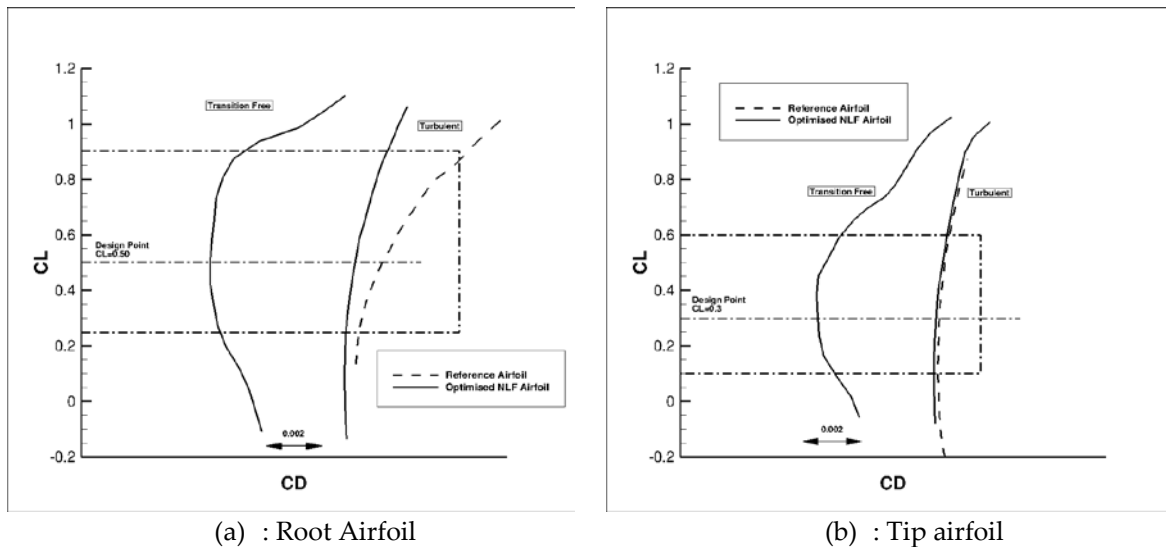


130
 131 **Figure 9 :** Reference TP90 aircraft (Leonardo).

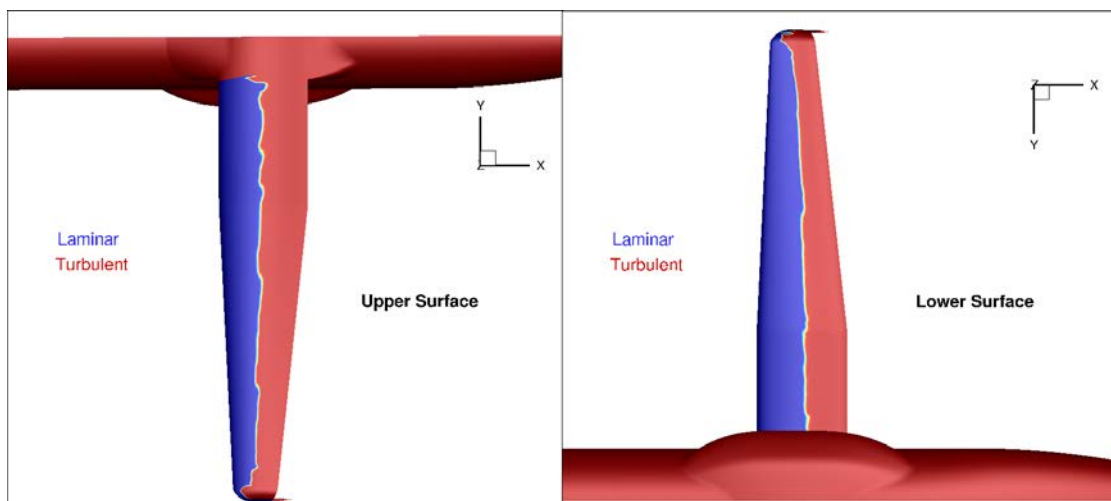
132 The wing airfoils were redesigned by ONERA at cruise conditions for Natural Laminar Flow
 133 capabilities, but the wing planform was not modified. The design considered a multi-point
 134 optimization of the tip and root airfoils for cruise, climb and low-speed conditions, in order to have a
 135 satisfactory performance level on a large part of the flight domain through an extended natural
 136 laminar flow on the upper and lower surfaces. Some details about the NLF wing design are given in
 137 [16]. Here, only main results are recalled. This configuration is referred as AG2-NLF in the
 138 following.

139 Figure 10 presents the two-dimensional computed performance of the re-designed root and tip
 140 airfoils of the AG2-NLF wing at nominal cruise conditions ($M=0.52$, Altitude=20000 ft). Performances
 141 of the reference (turbulent) airfoil at the same conditions are indicated. The new airfoils exhibit NLF
 142 characteristics on a large range of local C_L around the design value. In addition, the performance of

143 these airfoils in turbulent conditions are similar (a tip) or event better (at root) than for the reference
 144 one. Then, the wing has been generated considering these two airfoils and twist was adapted in
 145 order to take low speed performance into account, with no impact on the computed laminar flow
 146 extent on both surfaces at the design point (Figure 11).
 147



148 **Figure 10** : Root and Tip airfoil performance of the AG2-NLF wing at nominal cruise
 149 conditions.



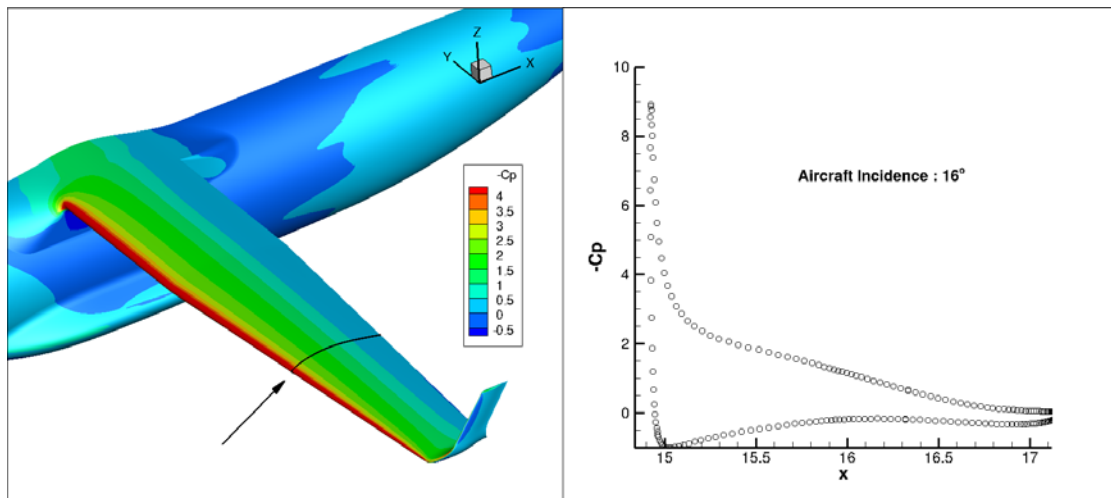
150 **Figure 11** : AG2-NLF wing at nominal cruise conditions – Computed extension of laminar
 151 flow on the wing surfaces.
 152

153 In a second phase of the project, some high-lift devices have been designed and adapted to this
 154 wing. Considering the high level of performance required at low speed, the use of morphing
 155 technology was mandatory for both leading-edge and trailing-edge devices.

156 **4. Use of a drooped nose**

157 Figure 12 presents the computed pressure distribution at low speed conditions ($M=0.15$ at sea
 158 level) for the clean AG2-NLF wing case. It can be seen that a significant pressure peak is found on
 159 the wing at high incidence. This is a common behavior observed for wing designed in order to have
 160 laminar flow characteristics (NLF or HLFC technologies) at cruise. In that case, the airfoil
 161 leading-edge radius is reduced compared to a turbulent one, in order to drive the favorable pressure
 162 gradient to maintain the flow laminar. The drawback is that at high angles of incidences, a strong
 163 acceleration is found at the airfoil leading edge that will increase the risk of leading-edge stall

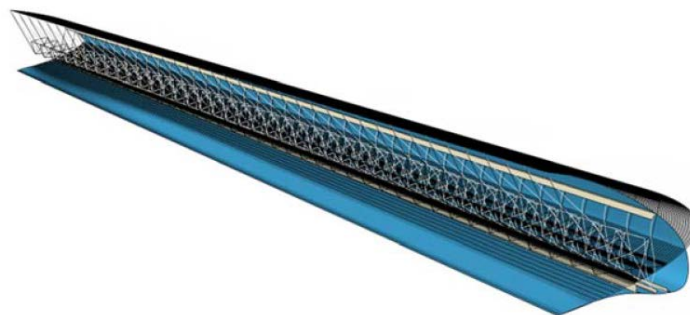
164 occurrence. It is therefore necessary to use a leading-edge device in order to act on the pressure peak
 165 at low speed conditions. Moreover, this device has to be compatible with the constraint of keeping
 166 laminar flow at cruise conditions when not deployed, and the morphing drooped nose device was
 167 retained.
 168



169
 170 **Figure 12:** AG2-NLF wing at low speed: development of a large suction peak at
 171 leading-edge.

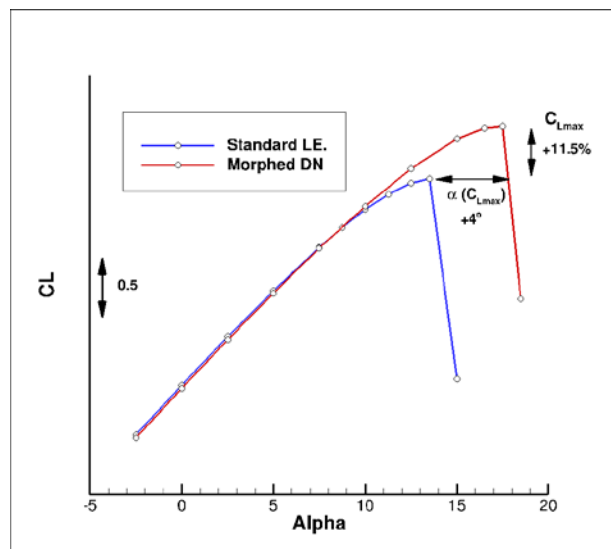
172 Moreover, compared with a standard droop nose, a morphing droop nose allows redesigning
 173 the baseline wing shape that can be optimized considering only the flight conditions that does not
 174 require the shape changes introduced by the morphing. This aspect provides an additional
 175 advantage in terms of aerodynamic benefit because different external shapes can be defined to
 176 optimize the aerodynamic performances in different flight conditions. The different shapes can be
 177 designed separately considering that the morphing allows the transition between them, preserves
 178 the shape continuity and avoids any type of step and gap. This advantage is greater in the case of
 179 laminar wing where the NLF wing can be optimized for the high-speed conditions and the same
 180 wing, equipped with the morphing droop nose, for the low-speed conditions.

181 The detailed process considered for the design of the droop nose adapted to the AG2-NLF wing
 182 can be found in [16][17][18]. It considered aero-structural optimizations carried out by Politecnico di
 183 Milano and aerodynamic performance assessments done by ONERA. First, a preliminary
 184 performance assessment has been done in two dimensional flow for a pre-designed landing
 185 configuration considering a standard flap. Figure 14 presents the computed $C_L(\alpha)$ curves for a
 186 geometry considering a droop nose or not. As for any leading edge devices, the use of a droop nose
 187 leads to an increase of maximum lift and stall angle, but with nearly no effect on the lift level for
 188 lower incidences. Values indicated for the gains (+11.5% in C_{Lmax} and +4° in stall angle) are for
 189 information only, as they are based on a 2D airfoil, and not on the 3D wing.
 190



191
 192 **Figure 13 :** Final 3D drooped nose designed by PoliMi [18].

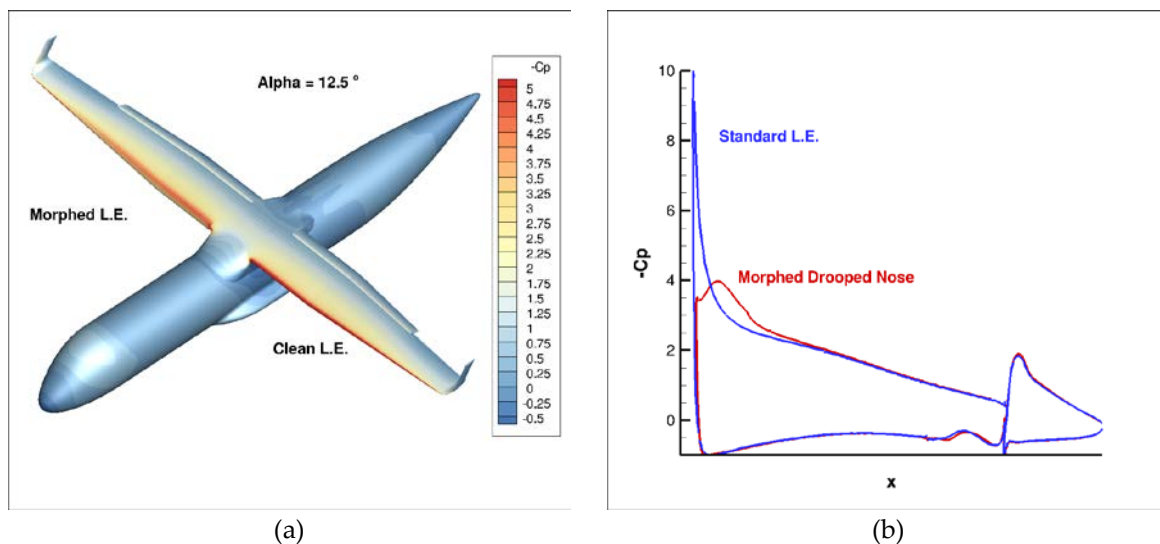
193



194

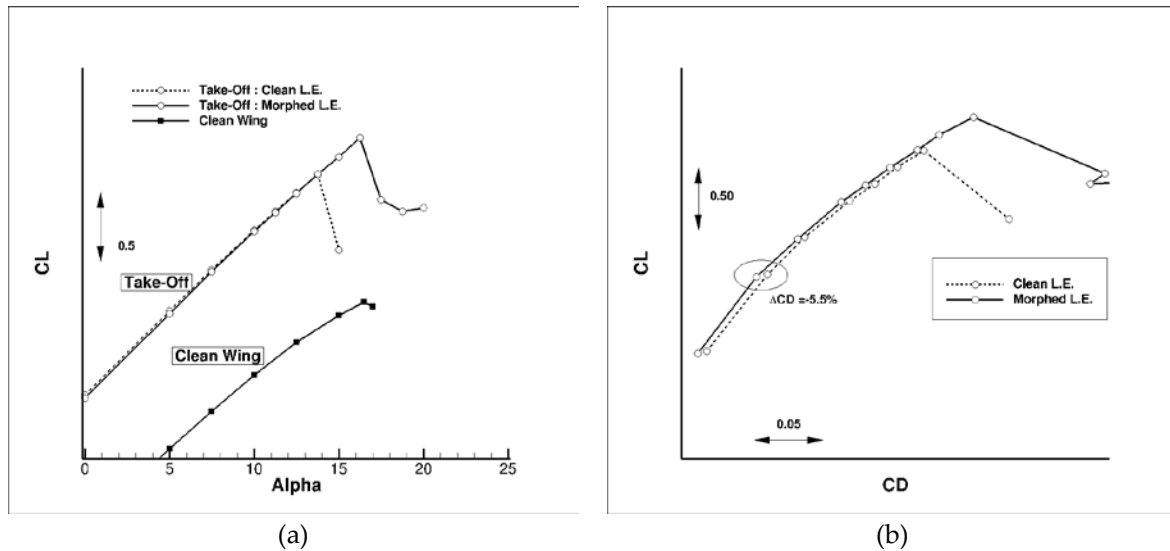
195 **Figure 14** : Use of a morphed drooped nose device – 2D Evaluation of $C_L(\alpha)$ curves –
 196 Landing conditions.

197 Different drooped nose shapes have been compared leading to the selection of a geometry that
 198 has been adapted to the 3D wing-body configuration for a CFD evaluation of the performances.
 199 Figure 15 compares the pressure distributions computed on the AG2-NLF airplane at take-off
 200 conditions ($M=0.20$ at sea level) for an incidence of 12.5° . The use of a drooped nose decreases
 201 significantly the suction peak at leading edge, which makes the pressure gradient less favorable for a
 202 leading-edge stall occurrence. Therefore, stall will occur at a higher incidence, as observed in Figure
 203 16(a).
 204



205 **Figure 15** : Effect of a drooped nose on pressure distribution (Take-off configuration,
 206 $\text{Alpha}=12.5^\circ$). Pressure distribution on the wing (a) and at the outboard flap section (b).

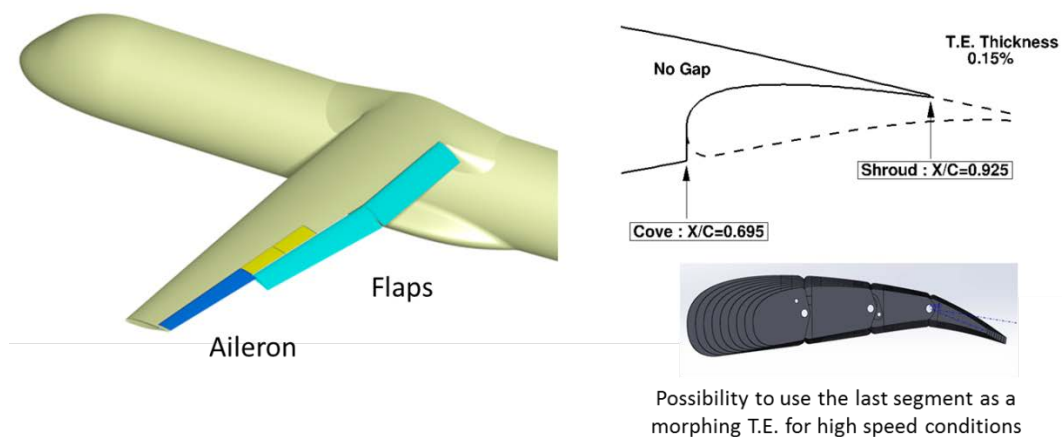
207 There is another (favorable) effect observed on drag. The change in pressure distribution at the wing
 208 leading-edge leads a constant decrease in drag coefficient, corresponding to a reduction of about
 209 5.5% at flight condition for the wing-body configuration.



210 **Figure 16** : Effect of a drooped nose on performance at take-off conditions. (a) $C_L(\alpha)$ curve ,
 211 (b) $C_L(C_D)$ curve.

212 **5. Use of a multi segmented flap system**

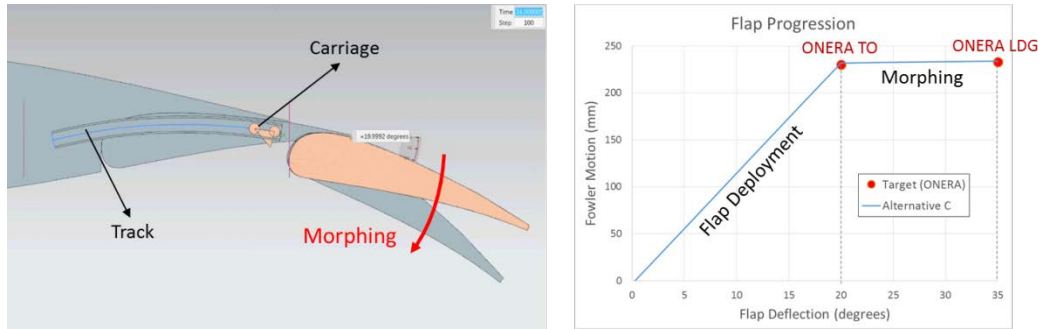
213 Among the different possibility to deform a wing for performance improvement, one
 214 considers multifunctional wing trailing edge. Such system acts on local wing shape deformations in
 215 order to modify the span load distribution. Detailed information about the design of the reference
 216 flap system used on the AG2-NLF wing are given in [16] and [19]. However, its spanwise extension
 217 corresponds to the place dedicated to trailing edge flaps (Figure 17). This system has therefore to be
 218 integrated to the flap, which leads to constraints for the design of the high-lift system. Considering
 219 the multi-segmented flap system retained, the use of the last segment as morphing device when flap
 220 is stowed leads to a maximum shroud location at 92.5% on the wing upper surface. Location of the
 221 cove on the lower surface is driven by wing structure rear spar location.
 222
 223



224
 225 **Figure 17** : General layout of the AG2-NLF wing for flap arrangements and flap design
 226 constraints.

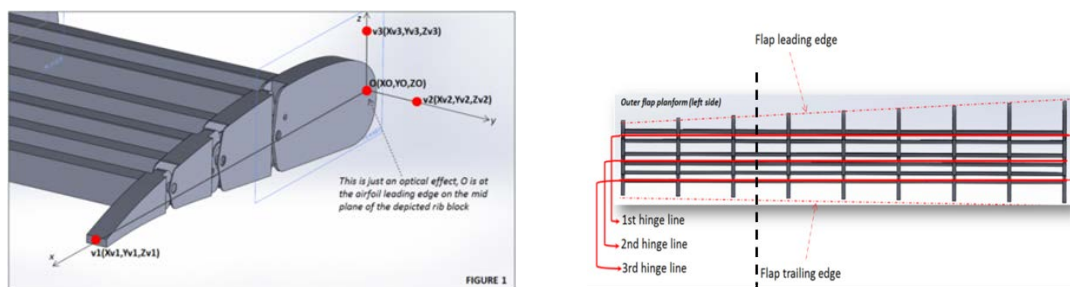
227 As mentioned in [16], it is possible to find an optimal aerodynamic setting for landing
 228 conditions when considering the rigid flap shape used for take-off. Different flap
 229 deployment progression laws were investigated by Siemens Industry Software NV [20]
 230 [21], who was responsible of the flap actuation system in the project, and evaluated by
 231 ONERA, but it was not possible to find a kinematic that will ensure take-off and landing
 232 settings that will not need an external fairing. However, it was possible to design fully

233 integrated tracking system to set the flap at the optimized take-off configuration. It was
 234 therefore decided to investigate the possibility to deform the flap shape by the use of
 235 morphing in order to obtain “sufficient” aerodynamic performance for landing conditions
 236 (Figure 18). Note that it is not evident that such process would necessarily works as we
 237 start from a take-off setting and shape (for the front flap segment) that are parameters
 238 usually to be optimized for landing conditions.



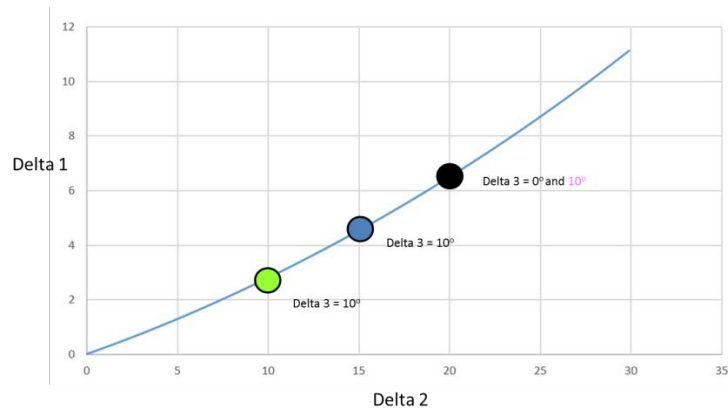
239
 240 **Figure 18** : Best alternative for a solution with no external fairing: Take-off configuration,
 241 then apply morphing for landing (Siemens).

242 Figure 19 presents the morphing flap system from UniNa adapted to the AG20-NLF wing
 243 geometry. Note that the different hinge lines are parallel to the flap trailing edge, and not at a
 244 constant local chord. It means that when deformation is applied, the flap shape is 3D and that the
 245 performance evaluation considering a 2D wing section is not possible. Three-dimensional numerical
 246 evaluations are mandatory.



247 **Figure 19** : Trailing edge morphing flap: general layout from UniNa.

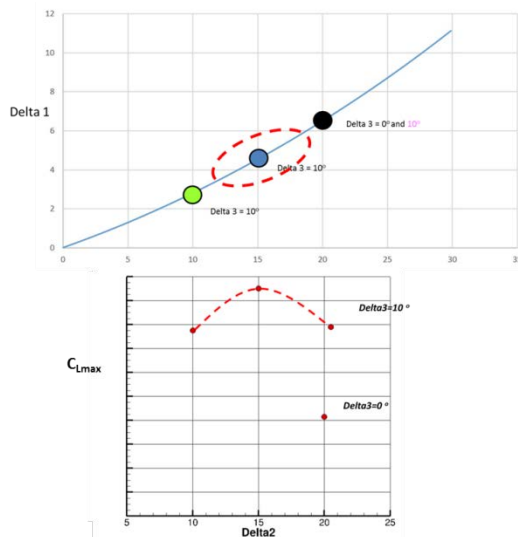
248 Due to mechanical constraints, there are some physical links existing between hinge 1 and 2
 249 leading to the kinematic law presented in Figure 20 for the rotation angles between these two hinges.
 250 For instance, it means that applying 5° deflection at hinge 1 leads to 15° at hinge 2 as a global
 251 deflection value (or $+10^\circ$ applied at hinge 2 after the 5° deflection for hinge 1). Deflection values for
 252 hinge 3 are free, but limited to 10° in amplitude. The symbols correspond to the configurations that
 253 have been evaluated numerically. Indeed, preliminary studies carried out based on the rigid flap
 254 shape gave an optimum flap deflection around 35° for landing. Taking into account the initial flap
 255 deflection of 20° , corresponding to the take-off case, we have to investigate configurations with a
 256 deflection angle of the second hinge around 15° .
 257



258

259 **Figure 20** – Morphing mechanism: Kinematic law for the rotation values at Hinge 1 and
 260 Hinge 2. Rotation at Hinge 3 is free. Symbols correspond to configurations considered for
 261 morphed flap at LDG conditions.

262 Based on results presented in Figure 21, the best combination for maximum lift optimization
 263 corresponds to a deflection of 15° for the second hinge, and a 10° extra deflection for the last segment.



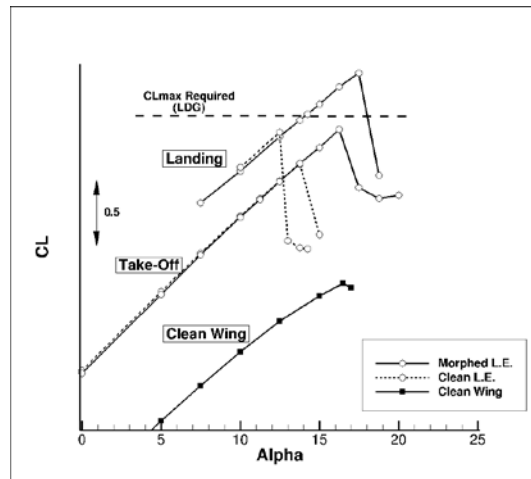
264

265 **Figure 21** : Optimization of the flap morphing system for landing.

266 The final performance assessment for the landing configuration ($M=0.150$ at sea level)
 267 considered the use of the drooped nose designed previously in combination with the deformable
 268 flap. Figure 22 compares the computed performance for both cases. It can be seen that the combined
 269 used of these two morphing devices leads to a significant improvement in both C_{Lmax} and stall angle.
 270 The requirement in term of C_{Lmax} level is respected, whereas it is not reached for the configuration
 271 equipped with the standard leading-edge.

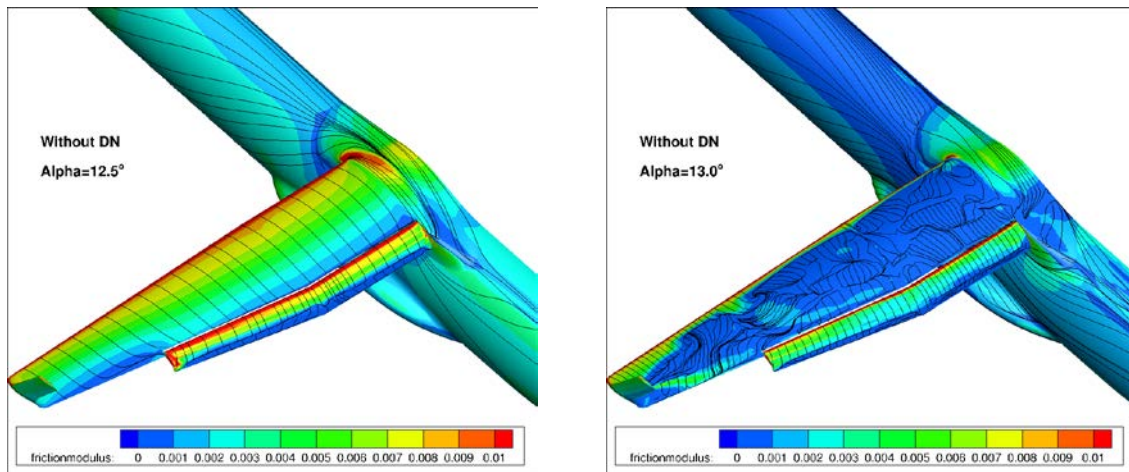
272 A final verification considered the stall process of the wing equipped with the drooped nose. It
 273 was asked to verify that there is no separation onset in the aileron area for flight control
 274 considerations. Figure 23 presents the computed skin friction lines for the landing configuration
 275 with the standard leading-edge. It can be seen that a separation occurs on the complete wing upper
 276 surface at stall. Figure 24 presents similar plots for the configuration equipped with the dropped
 277 nose. Stall occurs more gradually, and starts from the wing-body junction.

278



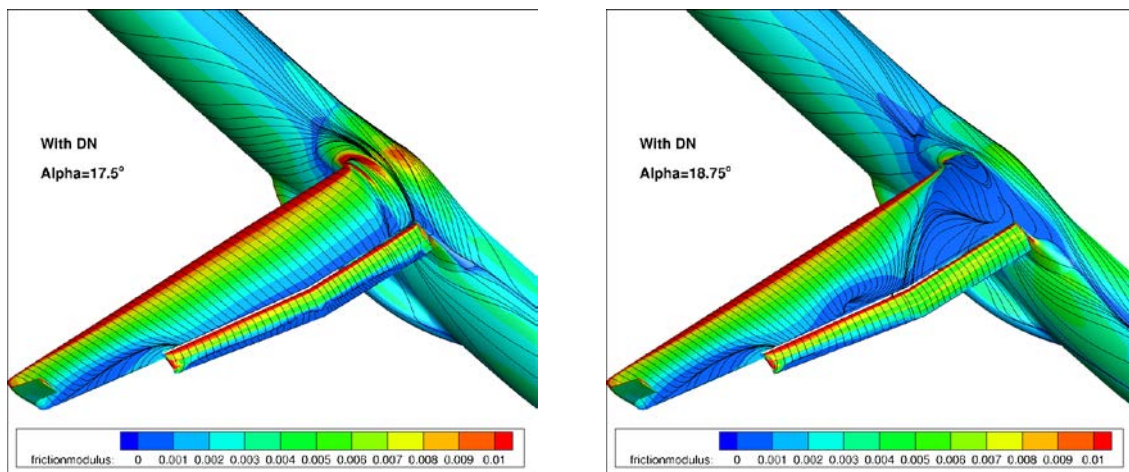
279
280
281

Figure 22 : High lift performance of the AG2-NLF equipped deformable elements (drooped nose and multi-segmented flap system).



282

Figure 23 : Landing configuration: stall process with standard leading-edge.



283

Figure 24 : Landing configuration: stall process with drooped nose leading-edge device.

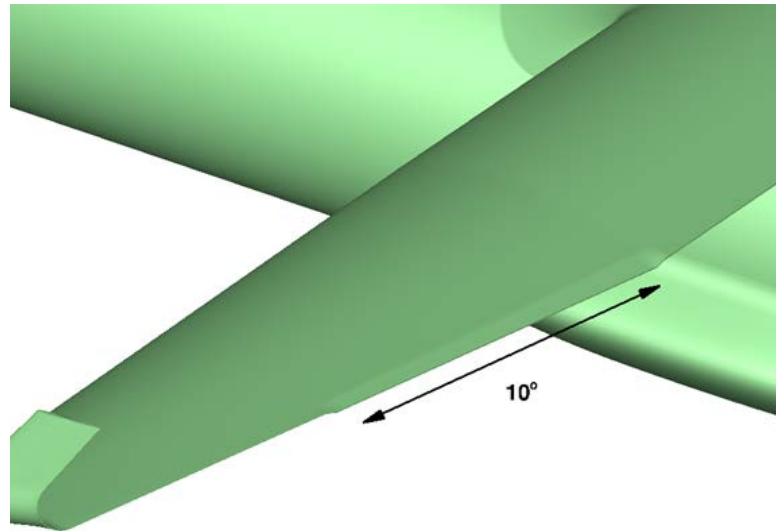
284

6. Use of flap morphing system for performance improvement in climb conditions

285
286
287
288

For the AG2-NLF regional airplane, multifunctional twistable trailing-edge could help to recover the laminar extent by an adaptation of pressure gradient in off-design condition [19]. Considering the C_L related to high speed climb condition ($M=0.36$, Altitude 15000 ft), free transition computations show that laminar flow on the upper surface starts to be lost on the outer wing. It was

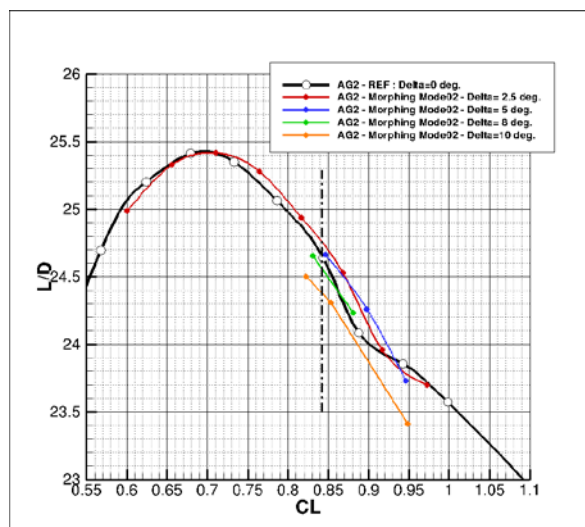
289 therefore investigated the possibility to deflect the last segment of the multi functional flap in order
 290 to improve performance in these conditions. Different tab deflections have been considered (2.5° ,
 291 5°, 8° and 10°). For the performance evaluations by CFD, the surface grid used for cruise evaluation
 292 has been deformed in the tab region and a mesh deformation technique, similar to the one used in
 293 the SARISTU project and described in [2], has been used. Figure 25 shows such configuration with a
 294 tab deflection of 10°.
 295



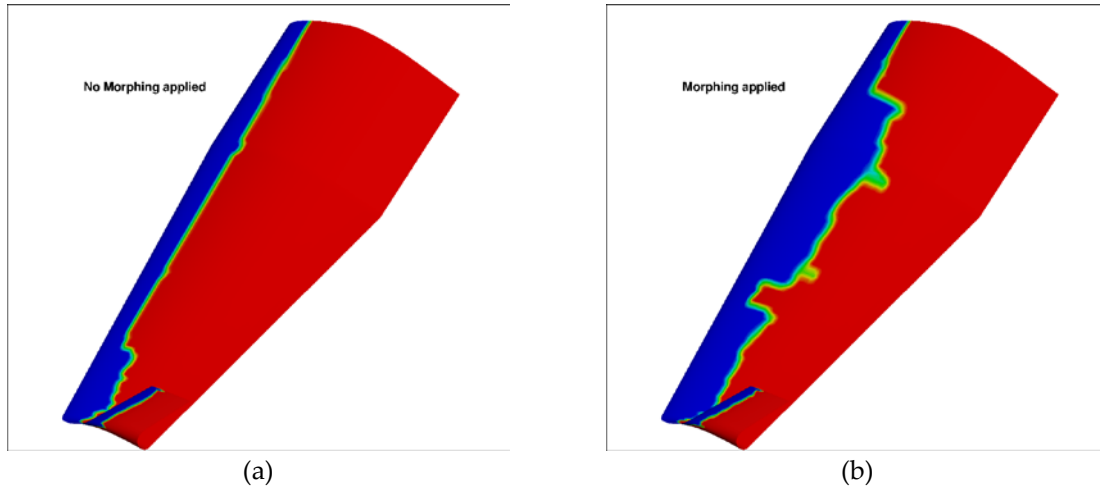
296
 297 **Figure 25** : Configuration considered for multi functional flap at climb conditions
 298 (example: deflection of 10°).

299 Figure 26 presents the computed LoD for the wing-body configuration of the AG2-NLF airplane
 300 for climb conditions. The black curve corresponds to the performance of the reference wing. For
 301 these conditions, the aircraft C_L is around 0.84/0.90. For these conditions, a loss of performance is
 302 observed due to the loss of laminar flow on the wing upper surface (Figure 27 (a)).

303 The use of small tab deflections (2.5° or 5°) allows recovering part laminar flow on the wing
 304 upper surface (Figure 27 (b)) and shifts the LoD curve to higher C_L values and increases the
 305 performance of about 2%. However, higher deflection angles (8° and 10°) lead to a global decrease of
 306 performance. When considering the drag breakdown between friction and pressure components
 307 (Figure 28), it can be seen that if an increase of tab deflection leads to a continuous decrease of
 308 friction drag, there is an increase of pressure drag that is associated, leading to an optimum value for
 309 low tab deflections.

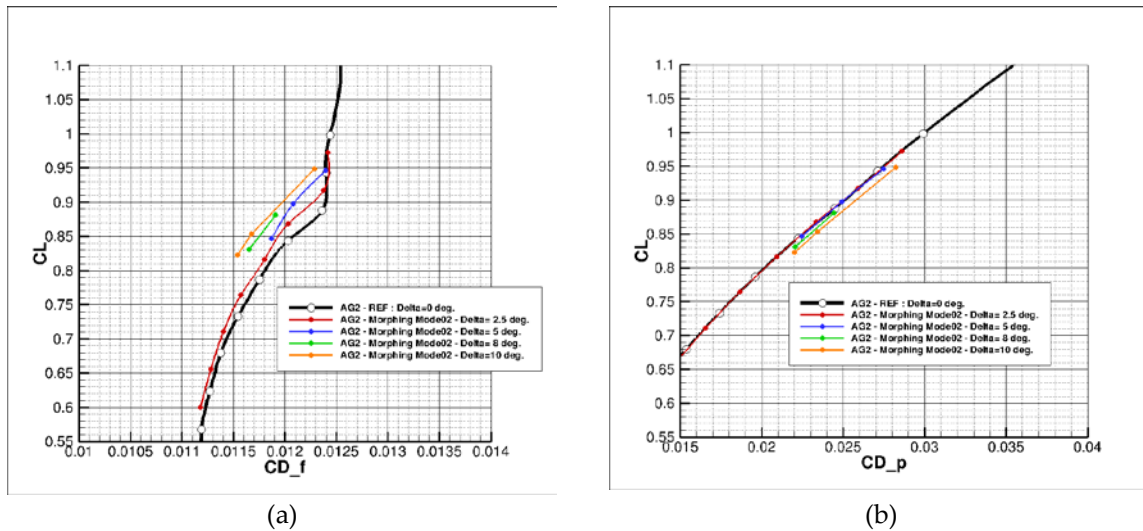


310
 311 **Figure 26** : Performance of the multi functional trailing edge flap (climb conditions).



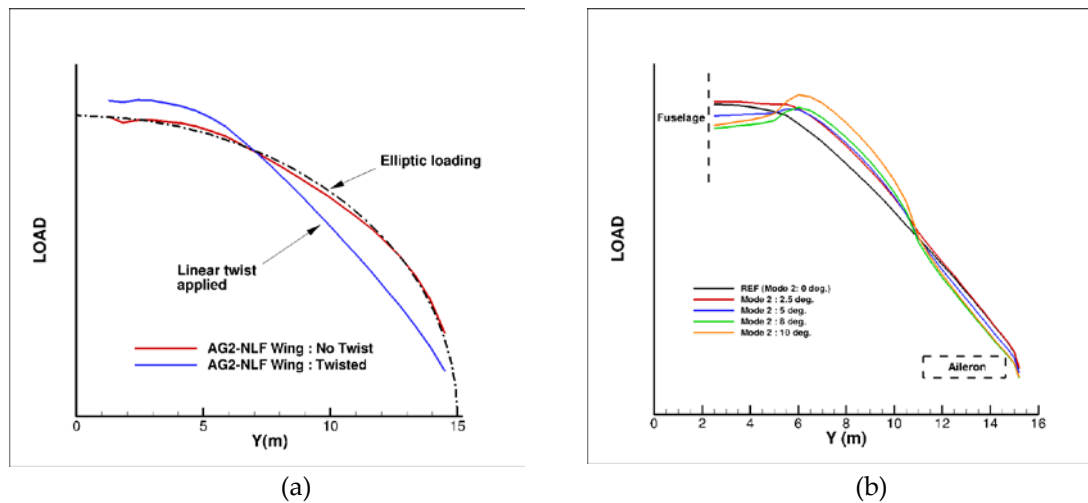
312 **Figure 27** : Natural laminar flow extent on the wing upper surface for climb conditions. (a)
 313 Reference wing (no morphing), (b) Morphing applied (2.5° deflection). Laminar flow in blue,
 314 Turbulent in red.

315



316 **Figure 28** : Drag breakdown for the different configuration of multi functional trailing
 317 edge flap (climb conditions). (a) Friction drag, (b) Pressure drag.

318 Finally, Figure 29 compares the different wing span load evolution at the design point in climb
 319 conditions for the different configurations considered. It can be seen that the baseline does not have
 320 an elliptic distribution, due to twist optimization for low speed considerations (Figure 29-(a)). The
 321 twist of the outer part of the wing has been optimized in order to shift the stall onset outside the
 322 aileron area at low speed conditions. A linear twist of 4° between the kink and the tip has been
 323 obtained. For the untwisted wing, a nearly elliptical span loading was achieved. The application of a
 324 linear twist on the outer wing leads to nearly linear variation of the span load, which will imply a
 325 degradation of lift induced drag component through the Oswald factor. Applying a deflection to the
 326 multi functional flap system has an effect on the span load evolution (Figure 29-(b)) but only in the
 327 portion where the system is located. Recovering an elliptic span loading would mean to act on the
 328 outer part of the outer wing, where the aileron is present. Therefore, gains on lift induced drag are
 329 not possible if there is no action in this area, through an aileron deflection(or morphed aileron) or a
 330 spanwise extension of the multi functional flap system up to tip.
 331



332 **Figure 29** : Computed wing span load evolution for the different configurations of the
 333 AG2-NLF wing. (a) Reference wing at nominal cruise flight conditions, (b) multi functional
 334 trailing edge flap deflected in climb conditions.

335 8. Conclusions

336 Aerodynamic performance for take-off and landing phases of a regional turboprop
 337 configuration equipped with a NLF wing have been significantly enhanced by the application of
 338 morphing technology for high lift devices. The use of a deformable morphing based drooped nose as
 339 leading edge device has been considered as it preserves the surface quality when retracted in cruise
 340 conditions. This device leads to an increase of both $C_{L,max}$ and stall angle.

341 For the trailing edge device, a multi segmented flap has been considered. For low speed
 342 applications, the objective was to obtain a mechanism that will not require any external fairing,
 343 which will improve significantly the drag at cruise. Different strategies have been considered in an
 344 interactive process between the partners involved (namely UniNa for the segmented flap system,
 345 Siemens for the definition of the tracking system and ONERA for the aerodynamic performance
 346 assessment), and it was found that an integrated tracking system was possible to set the flap at its
 347 take-off optimum location. Then, morphing was applied on the flap in order to reach the
 348 performance required for landing conditions.

349 Finally, the idea to use the flap last segment as morphing device for performance improvements
 350 in climb conditions has been verified. However, this performance improvement was obtained by a
 351 reduction of the friction drag, thanks to an adaptation of the laminar flow on the wing upper surface
 352 to flight conditions. It is therefore not sure that such performance improvement can be found when
 353 considering turbulent wings.

354 In this article, we only talked about aerodynamic performance improvements for the
 355 wing-body reference configuration. Of course, each component (drooped nose, flap system) has to
 356 be optimized in order to take into account the weight balance, the system complexity and aeroelastic
 357 behavior, and to be integrated into the complete aircraft architecture. Then further design phases can
 358 start by considering the propulsion system (nacelle, engines, propellers), the control surfaces
 359 (ailerons, horizontal tail, fin), the mechanical components (track systems), the structure and the
 360 energy sources. All these elements have to be integrated and considered for a complete aircraft
 361 performance on the complete flight envelope.

362 Finally, the use of morphing technology is not restricted to pure aerodynamic performance
 363 improvements. The use of deformable structures for load control during flight is another important
 364 application of this technology (see [22] for instance) ... and was their first use in the aviation history.

365

366 **Funding:** Part of the research described in this paper has been carried out in the framework of AIRGREEN2
 367 Project, which gratefully received funding from the Clean Sky 2 Joint Undertaking, under the European's Union
 368 Horizon 2020 research and innovation Program, Grant Agreement No. 807089—REG GAM
 369 2018—H2020-IBA-CS2-GAMS-2017.

370 **Acknowledgments:** The research leading to these results has received funding from the European
 371 Community's Seventh Framework Program (FP7/2007-2013) for the Clean Sky Joint Technology Initiative under
 372 grant agreement CSJU-GAM-GRA-2008-001 and the European Community's Horizon 2020 - the Framework
 373 Program for Research and Innovation (2014-2020) for the Clean Sky Joint Technology Initiative under grant
 374 agreement CS2-REG-GAM-2014-2015-01.

375 Special thanks goes to Sergio Ricci and Alessandro De Gaspari from Politecnico di Milano, Rosario Pecora from
 376 University of Naples "Federico II", Emre Ongut and Yves Lemmens from Siemens PLM, Ignazio Dimino from
 377 Italian Aerospace Research Centre (CIRA) and Giovanni Carossa from Leonardo Company.

378 **Conflicts of Interest:** "The author declares no conflict of interest."

379 References

- 380 1. https://commons.wikimedia.org/wiki/File:Leonardo_Design_for_a_Flying_Machine,_c._1488.jpg .
- 381 2. A. Concilio, I. Dimino, L. Lecce, R. Pecora: *Morphing Wing Technologies. Large Commercial Aircraft and Civil*
 382 *Helicopters*. Butterworth-Heinemann (Elsevier) 2018, ISBN: 978-0-08-100964-2.
- 383 3. https://fr.wikipedia.org/wiki/Clément_Ader .
- 384 4. http://www.wright-brothers.org/Information_Desk/Help_with_Homework/Wright_Photos/Wright_Photos.htm .
- 385 5. <http://www.airliners.net/photo/Santos-Dumont-Demoiselle/1524755/L> .
- 386 6. https://en.wikipedia.org/wiki/File:F-111A_Wing_Sweep_Sequence.jpg .
- 387 7. S.B. Smith, D.W. Nelson: *Determination of the aerodynamic characteristics of the mission adaptive wing*. AIAA
 388 journal of Aircraft, Vol 27 N°11, 1990 , pp 950-958.
- 389 8. <https://www.dfrc.nasa.gov/Gallery/Photo/F-111AFTI/index.html> .
- 390 9. A.H. Bowers, O.J. Murillo, R. Jensen, B. Eslinger, C. Gelzer: *On Wings of the Minimum Induced Drag: Spanload Implications for Aircraft and Birds*. NASA/TP -2016-219072, March 2016.
- 391 10. R. Hibig, H. Koerner: *Aerodynamic Design Trends for Commercial Aircraft*. NASA TM -77976, January 1986.
- 392 11. M. Fischer, H. Friedel, H. Holthusen, B. Gölling, R. Emunds: *Low noise design trends derived from wind tunnel testing on advanced high-lift devices*. 12th AIAA/CEAS Aeroacoustics Conference (27th AIAA Aeroacoustics Conference) 8-10 May 2006, Cambridge, Massachusetts (USA), AIAA 2006-2562.
- 393 12. https://www.nasa.gov/centers/armstrong/multimedia/imagegallery/2014_achievements/ED14-0333-014.html .
- 394 13. A.M.O. Smith: *High-Lift Aerodynamics*. AIAA Journal of Aircraft Vol 12 N°6, June 1975, pp 501,530.
- 395 14. <http://www.atraircraft.com/products/list.html> .
- 396 15. https://hr.wikipedia.org/wiki/Datoteka:A380_singapore_airlines_takeoff_arp.jpg .
- 397 16. A. De Gaspari, F. Moens: *Aerodynamic Shape Design and Validation of an Advanced High-Lift Device for a Regional Aircraft with Morphing Droop Nose*. Hindawi, International Journal of Aerospace Engineering, 2019: <https://doi.org/10.1155/2019/7982168>.
- 398 17. A. De Gaspari, A. Gilardelli, S. Ricci, A. Airoidi, F. Moens: *Design of a Leading Edge Morphing Based on Compliant Structures for a Twin-Prop Regional Aircraft*. 2018 AIAA/AHS Adaptive Structure Conference, Kissimmee, Florida, AIAA 2018-1063.
- 399 18. A. De Gaspari, A. Gilardelli, S. Ricci, A. Airoidi, F. Moens: *Design of a Leading Edge Morphing Based on Compliant Structures in the Framework of the CD2-Airgreen2 Project*. SMASIS 2018-8246. SMASIS 2018 Conference , September 10-12 2018, San Antonio, Texas (USA).
- 400 19. F. Rea, F. Amoroso, R. Pecora, F. Moens: *Exploitation of a Multifunctional Twistable Wing Trailing-Edge for Performance Improvement of a Turboprop 90-Seats Regional Aircraft*. MDPI, Aerospace 2018, 5, 122. doi:10.3390/aerospace5040122.
- 401 20. A.E. Öngüt A, Y. Lemmens: *A Simulation Methodology for the Design of Trailing-Edge Flap Deployment Mechanism*. NAFEMS Americas (CAASE), Cleveland, June 2018
- 402 21. A.E. Öngüt, M. Esposito, M. Barile, Y. Lemmens: *Design of a Novel Trailing-Edge Flap Deployment Mechanism*. Aerodays 2019, Bucharest (Romania).
- 403
- 404
- 405
- 406
- 407
- 408
- 409
- 410
- 411
- 412
- 413
- 414
- 415
- 416
- 417

- 418 22. C. Liauzun, D. Le Bihan, J.-M. David, D. Joly, B. Paluch: *Study of Morphing Winglet Concepts Aimed at*
419 *Improving Load Control and the Aeroelastic Behavior of Civil Transport Aircraft*. ONERA Aerospace Lab Journal,
420 Aeroelasticity and Structural Dynamics, Issue 14, September 2018. <http://www.aerospacelab-journal.org/>
421
422



© 2019 by the authors. Submitted for possible open access publication under the terms and conditions of the Creative Commons Attribution (CC BY) license (<http://creativecommons.org/licenses/by/4.0/>).

423